

THE H α LUMINOSITY FUNCTION AND STAR FORMATION RATE AT $Z \approx 0.24$ BASED ON SUBARU DEEP IMAGING DATA¹

SHINOBU S. FUJITA², MASARU AJIKI², YASUHIRO SHIOYA², TOHRU NAGAO², TAKASHI MURAYAMA²,
YOSHIAKI TANIGUCHI², KAZUYOSHI UMEDA², SANAE YAMADA², MASAFUMI YAGI³, SADANORI
OKAMURA^{4,5}, AND YUTAKA KOMIYAMA⁶

Draft version November 11, 2018

ABSTRACT

We have carried out a deep imaging survey for H α emitting galaxies at $z \approx 0.24$ using a narrowband filter tuned with the redshifted line. The total sky area covered is 706 arcmin² within a redshift range from 0.234 to 0.252 ($\delta z = 0.018$). This corresponds to a volume of 3.9×10^3 Mpc³ when $\Omega_{\text{matter}} = 0.3$, $\Omega_{\Lambda} = 0.7$, and $H_0 = 70$ km s⁻¹ Mpc⁻¹ are adopted. We obtain a sample of 348 H α emitting galaxies whose observed emission-line equivalent widths are greater than 12 Å. We find an extinction-corrected H α luminosity density of $10^{39.65^{+0.08}_{-0.12}}$ ergs s⁻¹ Mpc⁻³. Using the Kennicutt relation between the H α luminosity and star formation rate, the star formation rate density in the covered volume is estimated as $0.036^{+0.006}_{-0.012}$ M $_{\odot}$ yr⁻¹ Mpc⁻³. This value is higher by a factor of 3 than the local SFR density.

Subject headings: galaxies: distances and redshifts — galaxies: evolution — galaxies: luminosity function, mass function

1. INTRODUCTION

The star formation rate density is one of the important observables for our understanding of galaxy formation and evolution. Madau et al. (1996) compiled the evolution of star formation rate (SFR) density, ρ_{SFR} , as a function of redshift from the local universe to high-redshift. It is known that ρ_{SFR} steeply increases from $z \approx 0$ to $z \sim 1$ (Gallego et al. 1995; Tresse & Maddox 1998, hereafter TM98; Songaila et al. 1994; Ellis et al. 1996; Lilly et al. 1996; Hogg et al. 1998). However, ρ_{SFR} appears to be flat beyond $z = 2$ (Madau, Pozzetti, & Dickinson 1998; Pettini et al. 1998; Steidel et al. 1999; Barger et al. 2000; Fujita et al. 2003a; see also Trentham, Blain, & Goldader 1999).

Although recent investigations have been devoted to new estimates of ρ_{SFR} at high redshift, it seems also important to provide new estimates in nearby universe because only several investigations have been available between $z \approx 0$ to $z \sim 1$. For example, ρ_{SFR} at $z \approx 0.2 - 0.3$ is based solely on the observation by TM98. In this Letter, we present a new estimate of ρ_{SFR} at $z \approx 0.24$ based on the largest sample (more than 300 galaxies) studied so far, which was obtained with Suprime-Cam on the Subaru Telescope.

Throughout this paper, magnitudes are given in the AB system. We adopt a flat universe with $\Omega_{\text{matter}} = 0.3$, $\Omega_{\Lambda} = 0.7$, and $h = 0.7$ where $h = H_0 / (100 \text{ km s}^{-1} \text{ Mpc}^{-1})$.

2. OBSERVATIONS AND DATA REDUCTION

We have made a very deep optical imaging survey of H α emitters at $z \approx 0.24$ in a sky area surrounding the SDSSp J104433.04–012502.2 at redshift of 5.74 (Fan et al. 2000; Djorgovski et al. 2001; Goodrich et al. 2001) using the Suprime-Cam (Miyazaki et al. 2002) on the 8.2 m Subaru telescope

(Kaifu 1998) at Mauna Kea Observatories. The Suprime-Cam consists of ten 2k \times 4k CCD chips and provides a very wide field of view; 34' \times 27'.

In this survey⁷, we used the narrow-passband filter, NB816, centered at 8150 Å with the passband of $\Delta\lambda(\text{FWHM}) = 120$ Å; the central wavelength corresponds to a redshift of 0.24 for H α emission. We also used broad-passband filters, B , R_C , I_C , and z' . All the observations were done under photometric condition and the seeing size was between 0.7 arcsec and 1.3 arcsec during the run.

The individual CCD data were reduced and combined using IRAF and the mosaic-CCD data reduction software developed by Yagi et al. (2002). Detail of flux calibration will be presented in Fujita et al. (2003b). The combined images for the individual bands were aligned and smoothed with Gaussian kernels to match their seeing sizes. The region contaminated by fringing pattern is masked. The final images cover a contiguous 706 arcmin² area with a PSF FWHM of 1.''4. A total volume of 3.9×10^3 Mpc³ is probed in our NB816 image. The net exposure times of the final images are 28, 80, 56, 86, and 600 minutes for B , R_C , I_C , z' , and NB816, respectively. The limiting magnitudes are $B = 26.6$, $R_C = 26.2$, $I_C = 25.9$, $z' = 25.3$, and NB816 = 26.0 for a 3σ detection on a 2.''8 diameter aperture.

Catalogues of the objects are made using SExtractor (Bertin & Arnouts 1996). The objects are detected using the *double-image mode*: the narrowband frame is used as a reference image for detection and then the flux is summed up in 14-pixel diameter apertures in all images. This aperture size is 2.''8, i.e., $2 \times \text{FWHM}$ of the stellar objects in the final image of R_C -band.

3. RESULTS

¹ Based on data collected at Subaru Telescope, which is operated by the National Astronomical Observatory of Japan.

² Astronomical Institute, Graduate School of Science, Tohoku University, Aramaki, Aoba, Sendai 980-8578, Japan

³ National Astronomical Observatory, Mitaka, Tokyo 181-8588, Japan

⁴ Department of Astronomy, Graduate School of Science, University of Tokyo, Tokyo 113-0033, Japan

⁵ Research Center for the Early Universe, School of Science, University of Tokyo, Tokyo 113-0033, Japan

⁶ Subaru Telescope, National Astronomical Observatory, 650 N.A'ohoku Place, Hilo, HI 96720

⁷ This survey is originally intended to search for Ly α emitters at $z \approx 5.7$ (Ajiki et al. 2002; Shioya et al. 2002).

3.1. Selection of NB816-Excess Objects

Since the central wavelength of the I_C is bluer than that of the NB816 filter, we calculated magnitude that we refer to as the “ I_z continuum”, using a linear combination ($I_z = 0.76I_C + 0.24z'$) of the I_C and z' flux densities; a 3σ photometric limit of $I_z \simeq 26.0$ in a $2''.8$ diameter aperture. This enables us to more precisely sample the continuum at the same effective wavelength as that of the NB816 filter. Following the manner of the previous surveys using narrowband filter and taking the scatter in the I_z -NB816 color and our survey depth into account, candidate line-emitting objects are selected with the criterion of I_z -NB816 $\geq \max(0.1, 3\sigma \text{ error of } I_z\text{-NB816})$; note that I_z -NB816 = 0.1 corresponds to $EW_{\text{obs}} \approx 12 \text{ \AA}$. We compute the 3σ of the color as $3\sigma_{I_z\text{-NB816}} = -2.5 \log(1 - \sqrt{(f_{3\sigma_{\text{NB816}}})^2 + (f_{3\sigma_{I_z}})^2} / f_{\text{NB816}})$. This criterion is shown by the solid and dashed lines in Figure 1. There are 1224 sources that satisfy the above criterion. They are brighter than the limiting magnitude at each band.

3.2. Selection of NB816-Excess Objects at $z \approx 0.24$

A narrowband survey of emission line galaxies can potentially detect galaxies with different emission lines at different redshifts. If the source redshift and the rest frame wavelength of the line act to place it inside the narrowband filter, the line will be detected if it is sufficiently strong. The emission lines we would expect to detect are $H\alpha$, $H\beta$, $[\text{O III}]\lambda\lambda 4959, 5007$, and $[\text{O II}]\lambda 3727$ (Tresse et al. 1999; Kennicutt 1992b) as the narrowband filter passband is too wide to separate $[\text{N II}]\lambda\lambda 6548, 6584$ from $H\alpha$. In Table 1 we show the different redshift coverage for each line.

In order to distinguish $H\alpha$ emitters at $z \approx 0.24$ from emission-line objects at other redshifts, we investigate their broad-band color properties comparing observed colors of our 1224 emitters with model ones that are estimated by using the population synthesis model GISSSEL96 (Bruzual & Charlot 1993). In Figure 2, we show the $B-R_C$ vs. R_C-I_C color-color diagram of the 1224 sources and the loci of model galaxies. Then we find that $H\alpha$ emitters at $z \approx 0.24$ can be selected by adopting the following three criteria (see for detail, Fujita et al. 2003b); (1) $B-R_C > 2(R_C-I_C) + 0.2$, (2) $z'-\text{NB816} > 0$, and (3) $I_C-\text{NB816} < 0.75(z'-\text{NB816}) + 0.35$. These criteria give us a sample of 348 $H\alpha$ emitting galaxy candidates. In particular, the first color criterion is a quite nice discriminator between $H\alpha$ emitters at $z \approx 0.24$ and other emitters at different redshifts and thus it is expected that there is few contamination in our sample.

We adopt the same method as that used by Pascual et al. (2001) to calculate $H\alpha$ equivalent width. The flux density in each filter can be expressed as the sum of the line flux and the continuum flux density (the line is covered by both filters):

$$f_{\text{NB}} = f_C + \frac{F_L}{\Delta \text{NB}}, \text{ and } f_{I_z} = f_C + 0.76 \frac{F_L}{\Delta I} \quad (1)$$

with f_C the continuum flux density; F_L the line flux; ΔNB and ΔI the narrow and I_C band filter effective widths and f_{NB} and f_{I_z} the flux density in each filter. Then the line flux, continuum flux density, and equivalent width can be expressed as follows:

$$F_L = \Delta \text{NB} \frac{f_{\text{NB}} - f_{I_z}}{1 - 0.76(\Delta \text{NB}/\Delta I)}, \quad (2)$$

$$f_C = \frac{f_{I_z} - 0.76 f_{\text{NB}} (\Delta \text{NB}/\Delta I)}{1 - 0.76(\Delta \text{NB}/\Delta I)}, \quad (3)$$

$$EW_{\text{obs}} = \frac{F_L}{f_C} = \Delta \text{NB} \left(\frac{f_{\text{NB}} - f_{I_z}}{f_{I_z} - 0.76 f_{\text{NB}} (\Delta \text{NB}/\Delta I)} \right), \quad (4)$$

where $\Delta I = 1269 \text{ \AA}$ for the I_C band and $\Delta \text{NB} = 120 \text{ \AA}$ for the NB816 band. The minimum line flux in our 348 sources is $1.2 \times 10^{-17} \text{ ergs s}^{-1}$ and the minimum continuum flux density reaches $3.0 \times 10^{-30} \text{ ergs s}^{-1} \text{ Hz}^{-1}$ (≈ 25.2 in AB magnitude).

3.3. $H\alpha$ Luminosity

In order to obtain the $H\alpha$ luminosity for each source, we correct for the presence of $[\text{N II}]\lambda\lambda 6548, 6584$ lines. Further, we also apply a mean internal extinction correction to each object. For these two corrections, we have adopted the flux ratio of $f(H\alpha)/f([\text{N II}]\lambda\lambda 6548, 6584) = 2.3$ (obtained by Kennicutt 1992a; Gallego et al. 1997; used by TM98; Yan et al. 1999; Iwamuro et al. 2000) and $A_{H\alpha} = 1$.

We also apply a statistical correction (28%; the average value of flux decrease due to the filter transmission) to measured flux because the filter transmission function is not square in shape. The $H\alpha$ flux is given by:

$$f_{\text{cor}}(H\alpha) = f(H\alpha + [\text{N II}]) \times \frac{f(H\alpha)}{f(H\alpha) + f([\text{N II}])} \times 10^{0.4A_{H\alpha}} \times 1.28. \quad (5)$$

We calculate $f(H\alpha + [\text{N II}])$ from the total magnitude; note that the aperture size is determined from the I_C -band image. Finally the $H\alpha$ luminosity is given by $L(H\alpha) = 4\pi d_L^2 f_{\text{cor}}(H\alpha)$ using the redshift of the line at the center of the filter $z = 0.242$ and the luminosity distance, d_L .

4. LUMINOSITY FUNCTION AND STAR FORMATION RATE

4.1. Luminosity function of $H\alpha$ emitters

In order to investigate the star formation activity in galaxies at $z \approx 0.24$, we construct the $H\alpha$ luminosity function (LF) for our $H\alpha$ emitter sample by using the relation, $\Phi(\log L(H\alpha)) \Delta \log L(H\alpha) = \sum_i 1/V^i$, where V^i is the comoving volume, and the sum is over galaxies with $H\alpha$ luminosity within the interval $[\log L(H\alpha) \pm 0.5 \Delta \log L(H\alpha)]$. We take account of the filter shape in the computation of the volume. The correction can be as large as 13% for the faint galaxies [$L(H\alpha) < 10^{41} \text{ ergs s}^{-1}$] as compared to that for the brightest galaxies. Figure 3 shows the result with the Schechter function (Schechter 1976) fit to the $z \lesssim 0.3$ $H\alpha$ LF measured by TM98 (which is characterized by $\alpha = -1.35$, $\phi_* = 10^{-2.56} \text{ Mpc}^{-3}$, and $L_* = 10^{41.92} \text{ ergs s}^{-1}$; note that we convert the parameters to those of our adopted cosmology).

Fitting $H\alpha$ LF of $L(H\alpha) > 10^{40} \text{ ergs s}^{-1}$ with a Schechter function, we find that the best-fitting parameters are $\alpha = -1.53 \pm 0.15$, $\log \phi_* = -2.62 \pm 0.34$, and $\log L_* = 41.95 \pm 0.25$. We find that the faint end slope of our LF is steeper than that obtained by TM98. This difference may be attributed to the different source selection procedures between TM98 and ours; i.e., TM98 used I -selected CFRS galaxies lying at redshift below 0.3 with the limiting magnitude of $I_{\text{AB}} = 22.5$, while we used NB816-selected galaxies with the much deeper limiting magnitude of $I_C \simeq 25$. In order to check this possibility, we have made LFs of $I_C < 24$, $I_C < 23$, and $I_C < 22$ sources (Figure 4), using our I_C -selected catalog. It is shown from this analysis that the LF for galaxies with a brighter I_C -band limiting magnitude tend to have a shallower faint end slope although the brightest end of LFs is not affected by the I_C -band limiting magnitude. The difference between LF of TM98 and our data is originated from

this point. In addition to this, our survey is concentrated in a small redshift range around $z \approx 0.24$ while the redshift range of TM98 is $z \leq 0.3$. This may also affect the LF shape. It should be noted that our result is consistent with that obtained by Pascual et al. (2001) although their data are available only for brighter objects with $\log L(\text{H}\alpha) \gtrsim 42$.

4.2. Luminosity density and star formation rate density

The H α luminosity density is obtained by integrating the LF:

$$\mathcal{L}(\text{H}\alpha) = \int_0^\infty \Phi(L) L dL = \Gamma(\alpha+2) \phi_* L_* \quad (6)$$

We then find a total H α luminosity per unit comoving volume $10^{39.65^{+0.08}_{-0.17}}$ ergs s $^{-1}$ Mpc $^{-3}$ at $z \approx 0.24$ from our best fit LF. The errors quoted here are the standard deviations taking into account that the three Schechter parameters are correlated. Our estimate is quite similar to that obtained by Pascual et al. (2001), $10^{39.79 \pm 0.09}$ ergs s $^{-1}$ Mpc $^{-3}$.

Not all the H α luminosity is produced by star formation, because active galactic nuclei (AGNs) can also contribute to the luminosity. The amount of this contribution depends on the selection criteria. For example, it is 8-17% in the CFRS low- z

sample (Tresse et al. 1996), 8% in the local UCM (Gallego et al. 1995), and 17-28% in the 15R survey (Carter et al. 2001) for the number of galaxies. Following the manner of Pascual et al. (2001), we adopt that AGNs contribute to 15% of the luminosity density. We correct this AGNs contribution and then obtain the corrected luminosity density, $10^{39.58^{+0.08}_{-0.17}}$ ergs s $^{-1}$ Mpc $^{-3}$.

The star formation rate can be estimated from the H α luminosity using $SFR = 7.9 \times 10^{-42} L(\text{H}\alpha) M_\odot \text{yr}^{-1}$, where $L(\text{H}\alpha)$ is in units of ergs s $^{-1}$ (Kennicutt 1998). Thus, the H α luminosity density can be translated into the SFR density of $\rho_{\text{SFR}} \simeq 0.036^{+0.006}_{-0.012} M_\odot \text{yr}^{-1} \text{Mpc}^{-3}$ (with AGN correction $0.031^{+0.005}_{-0.010} M_\odot \text{yr}^{-1} \text{Mpc}^{-3}$). Figure 5 shows the evolution of the SFR density from $z = 0$ to $z = 2.0$. The SFR density measured here is higher than that of TM98. This is mainly due to the difference of faint end slope as shown before. Our result is consistent with the strong increase in SFR density from $z = 0$ to $z \simeq 1$.

We would like to thank the Subaru Telescope staff for their invaluable help. We thank the referee, Jesus Gallego, for his detailed comments that improved this article. We also thank T. Hayashino for his invaluable help. This work was financially supported in part by the Ministry of Education, Culture, Sports, Science, and Technology (Nos. 10044052 and 10304013).

REFERENCES

- Ajiki, M., et al. 2002, ApJ, 576, L25
 Barger, A. J., Cowie, L. L., & Richards, E. A. 2000, AJ, 119, 2092
 Bertin, E., & Arnouts, S. 1996, A&AS, 117, 393
 Bruzual A., G & Charlot, S. 1993, ApJ, 405, 538
 Carte, B. J., Fabricant, D. G., Geller, M. J., Kurtz, M. J., & McLean, B. 2001, 559, 606
 Connolly, A. J., Szalay, A. S., Dickinson, M., Subbarao, M. U., & Brunner, R. J. 1997, ApJ, 486, L11
 Djorgovski, S. G., Castro, S., Stern, D., & Mahabal, A. A. 2001, ApJ, 560, L5
 Ellis, R. S., Colless, M., Broadhurst, T., Heyl, J., & Glazebrook, K. 1996, MNRAS, 271, 781
 Fan, X., et al. 2000, AJ, 120, 1167
 Fujita, S. S., et al. 2003a, AJ, 125, 13
 Fujita, S. S., et al. 2003b, in preparation
 Gallego, J., Zamorano, J., Aragón-Salamanca, A., & Rego, M. 1995, ApJ, 455, L1; Erratum 1996, ApJ, 459, L43
 Gallego, J., Zamorano, J., Rego, M., & Vitores, A. G. 1997, ApJ, 475, 502
 Goodrich, R. W., et al. 2001, ApJ, 561, L23
 Gronwall C., 1999, in Holt S., Smith E., eds, Proc. Conf. 'After the Dark Ages: When Galaxies were Young.' AIP, New York, p. 335
 Iwamuro, F., et al. 2000, PASJ, 52, 73
 Hopkins A. M., Connolly, A. J., & Szalay, A. S. 2000, AJ, 120, 2843
 Hogg, D. W., Cohen, J. G., Blandford, R., & Pahre, M. A. 1998, ApJ, 504, 622
 Kaifu, N. 1998, Proc. SPIE, 3352, 14
 Kennicutt, R. C. 1992a, ApJ, 388, 310
 Kennicutt, R. C. 1992b, ApJS, 79, 255
 Kennicutt, R. C. 1998 ARA&A, 36, 189
 Lilly, S. J., Le Fevre, O., Hammer, F., Crampton, D. 1996, ApJ, 460, L1
 Madau, P., Ferguson, H. C., Dickinson, M. E., Giavalisco, M., Steidel, C. C., & Fruchter, A. 1996, MNRAS, 283, 1388
 Madau, P., Pozzetti, L., & Dickinson, M. E. 1998, ApJ, 498, 106
 Miyazaki, S., et al. 2002, PASJ, 54, 833
 Moorwood, A. F. M., van der Werf, P. P., Cuby, J. G., & Oliva, E. 2000, A&A, 362, 9
 Pascual, S., Gallego, J., Aragón-Salamanca, A., & Zamorano, J. 2001, A&A, 379, 798
 Pettini, M., et al. 1998, in Cosmic Origins: Evolution of Galaxies, Stars, Planets, and Life, ed. J. M. Shull, C. E. Woodward, & H. A. Thronson (San Francisco: ASP), 67
 Schechter, P. 1976, ApJ, 203, 297
 Shioya, Y., et al. 2002, PASJ, 54, 975
 Steidel, C. C., Adelberger, K. L., Giavalisco, M., Dickinson, M., & Pettini, M. 1999, ApJ, 519, 1
 Songaila, A., Cowie, L. L., Hu, E. M., & Gardner, J. P. 1994, ApJS, 94, 461
 Sullivan, M., Treyer, M., Ellis, R. S., Bridges, B., & Donas, J. 2000, MNRAS, 312, 442
 Trentham, N., Blain, A. W., Goldader, J. 1999, MNRAS, 305, 61
 Tresse, L., & Maddox, S. 1998, ApJ, 495, 691 (TM98)
 Tresse, L., Maddox, S., Le Fèvre, O., & Cuby, J.-G. 2002, MNRAS, 337, 369
 Tresse, L., Maddox, S., Loveday, J., & Singleton, C. 1999, MNRAS, 310, 262
 Tresse, L., Rola, C., Hammer, F., Stasińska, G., Le Fèvre, O., Lilly, S. J., & Crampton, D. 1996, MNRAS, 281, 847
 Treyer, M. A., Ellis, R. S., Milliard, B., Donas, J., & Bridges, T. J. 1998, MNRAS, 300, 303
 Yagi, M., Kashikawa, N., Sekiguchi, M., Doi, M., Yasuda, N., Shimasaku, K., & Okamura, S. 2002, AJ, 123, 66
 Yan, L., et al. 1999, ApJ, 519, L47

TABLE 1
EMISSION LINES POTENTIALLY DETECTED INSIDE THE NARROWBAND.

Line	Redshift range $z_1 \leq z \leq z_2$		\bar{z}^a	d_L^b (Mpc)	$V \times 10^{4c}$ (Mpc ³)
H α	0.233	0.251	0.242	1220	0.39
[O III] $\lambda\lambda$ 4959,5007	0.616	0.640	0.628	3740	2.39
H β	0.664	0.689	0.677	4100	2.62
[O II] λ 3727	1.17	1.20	1.19	8190	7.30

^aMean redshift.

^bLuminosity distance.

^cComoving volume.

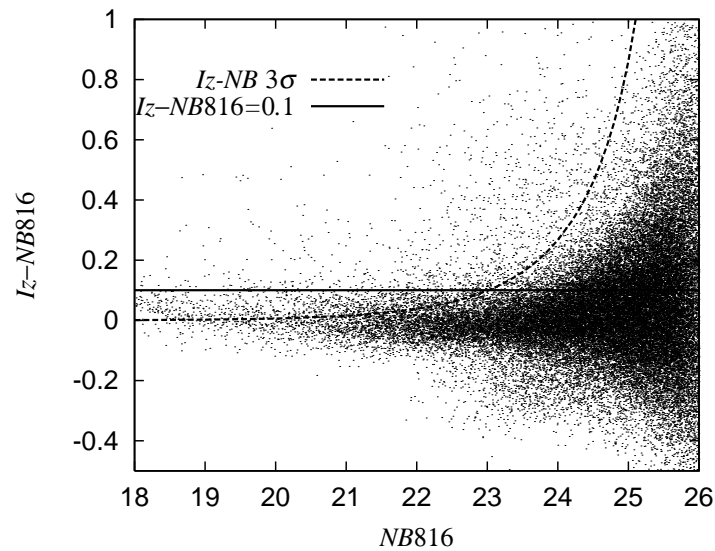


FIG. 1.— Objects detected down to $NB816 = 26$ in the $NB816$ -selected catalog. The horizontal solid line corresponds to $I_z - NB816 = 0.1$. Dashed line shows the distribution of 3σ error. Because bright sources are saturated in the continuum frame, $I_z - NB816$ is not zero at $NB816 \lesssim 19$.

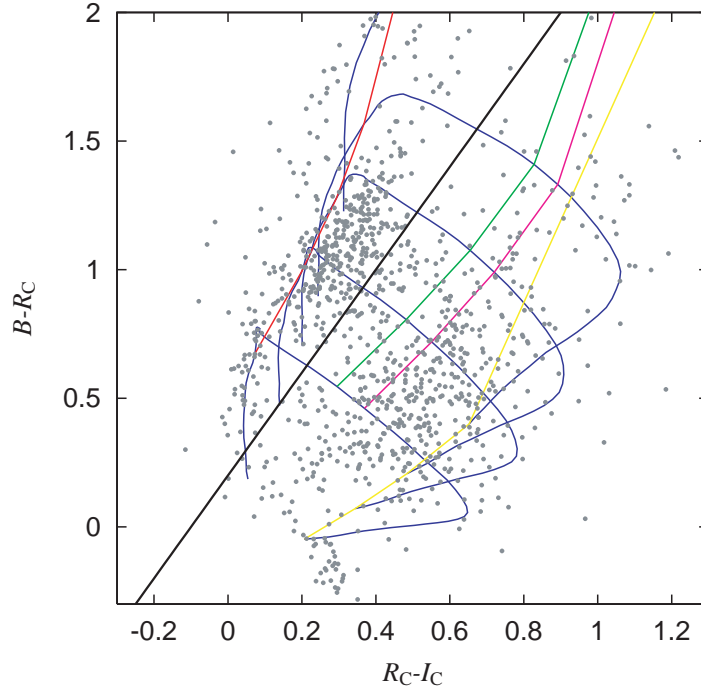


FIG. 2.— Plot of $B-R_C$ vs. R_C-I_C for the 1224 sources found with emitter selection criteria (gray circles). Colors of model galaxies (SB, Irr, Scd, Sbc, and E) from $z = 0$ to $z = 1.2$ are shown with blue lines. Colors of $z = 0.24, 0.64, 0.68,$ and 1.18 (for H α , [O III], H β , and [O II] emitters, respectively) are shown with red, green, purple, and yellow lines. We select the sources above the black line as H α emitters.

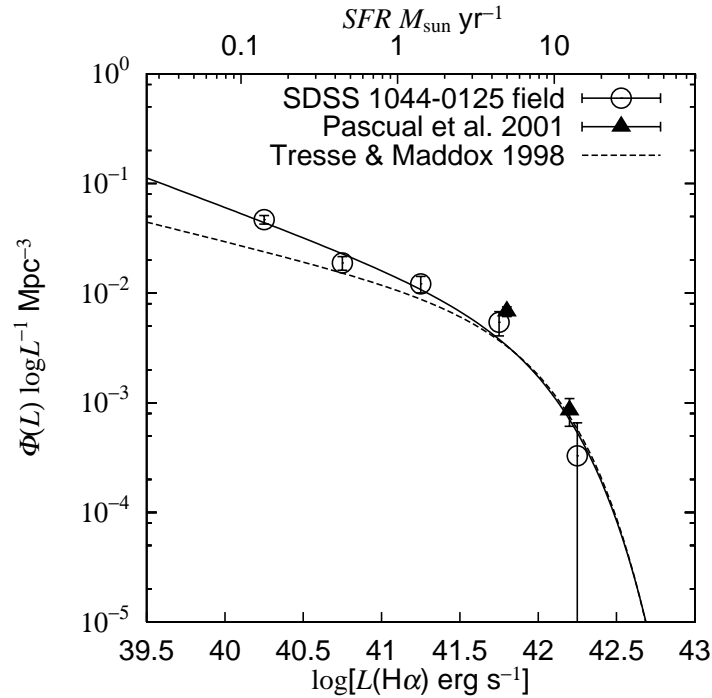


FIG. 3.— Luminosity function at $z \approx 0.24$ (open circles). Solid line is the best fitted Schechter function. The data points with $L(\text{H}\alpha) \geq 10^{40}$ ergs s^{-1} are used in the LF fitting. The TM98 H α luminosity function at $z \leq 0.3$ is shown with dashed line. The data points of Pascual et al. (2001) are also shown by filled triangles.

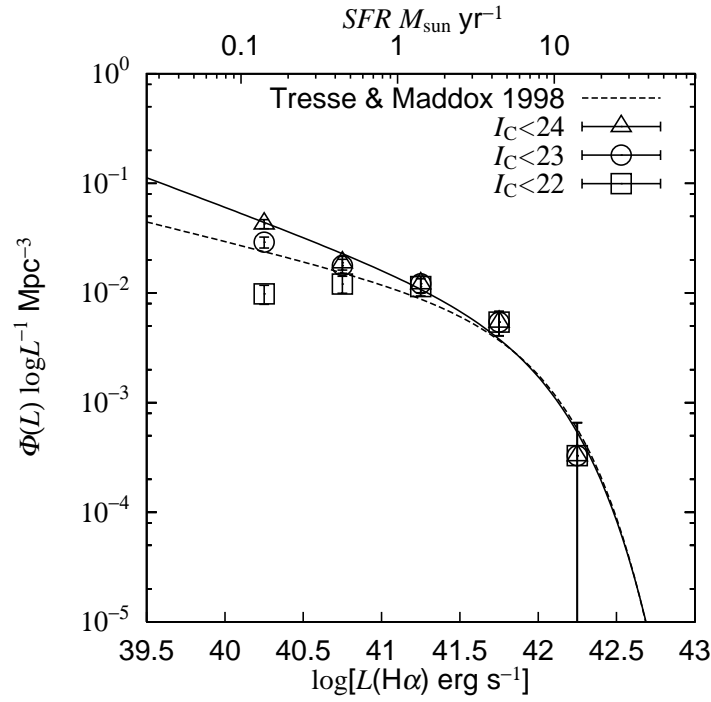


FIG. 4.— Effects of the threshold of I_C magnitude in our $H\alpha$ luminosity function. The solid and dashed lines have the same meanings as those in Figure 3. LFs of I_C -selected $H\alpha$ emitting galaxies are shown with triangles ($I_C < 24$), circles ($I_C < 23$), and squares ($I_C < 22$).

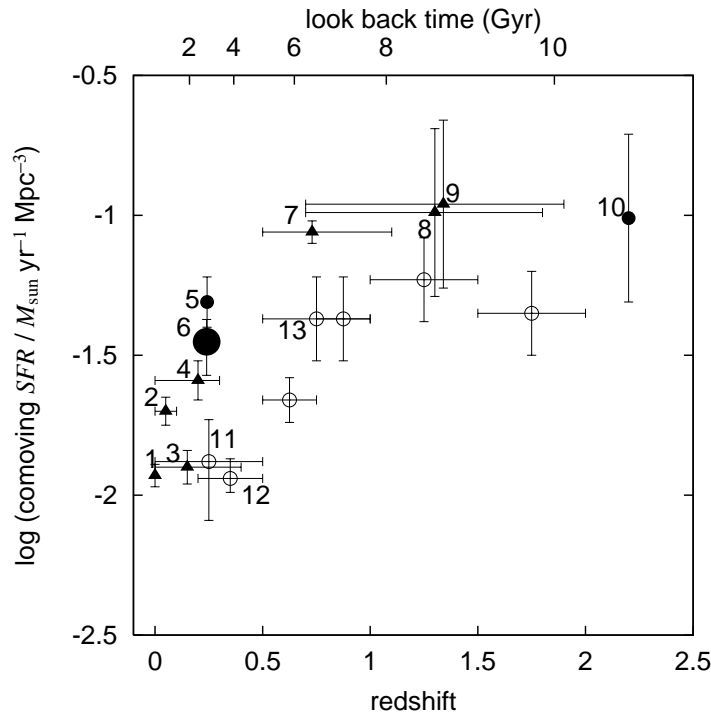


FIG. 5.— Star formation rate density at $z \approx 0.24$ derived from in this study (filled circle; ref. – 6) shown together with the previous investigations compiled by Trentham et al. (1999) and Tresse et al. (2002). Filled symbols show SFR derived from $H\alpha$ LFs obtained by spectroscopy (triangles) and narrowband imaging (circles). Open circles are SFR density derived from UV LFs which includes no dust correction. References: 1 – Gallego et al. (1995), 2 – Gronwall (1999), 3 – Sullivan et al. (2000), 4 – TM98, 5 – Pascual et al. (2000), 7 – Tresse et al. (2002), 8 – Hopkins et al. (2000), 9 – Yan et al. (1999), 10 – Moorwood et al. (2000), 11 – Treyer et al. (1998), 12 – Lilly et al. (1996), 13 – Connolly et al. (1997)